Supporting Information

Integrated Design of Functional Composite Electrolyte and Cathode for All-Solid-State Li Metal Batteries

Zhenghang Zhang,[1†] Rongzheng Fan,[1†] Saifang Huang,[1*] Jie Zhao,[1] Yudong Zhang,[1] Weiji Dai,[1] Cuijiao Zhao,[1]Xin Song,[2*] and Peng Cao[2]

[1]*School of Materials Science and Engineering, Jiangsu University of Science and Technology, Zhenjiang 212003, China*

[2] *Department of Chemical and Materials Engineering, The University of Auckland, Auckland 1142, New Zealand*

* Corresponding Authors: s.huang@just.edu.cn (S.H.), xson574@aucklanduni.ac.nz (X.S.)

† These authors contributed equally.

The lithium-ion transference number for the electrolytes was calculated by using the Bruce−Vincent method in **Equation S1:**

$$t_{\mathrm{Li}^+} = \frac{I_{ss} \times (V - I_0 R_0)}{I_0 \times (V - I_{ss} R_{ss})} \quad \text{(S1)}$$

where t_{Li^+} is the lithium-ion transference number, I_0 is the initial current, I_{ss} is the steady-state current, R_0 is the initial resistance measured before polarization, R_{ss} is the steady-state resistance obtained after polarization, and V is the applied polarization voltage.

Table S1. Potentiostatic polarization data of the Li/ DL@L /Li cell before and after cycling

V / mV	I_0 / mA	R_0 / Ω	I_{ss} / mA	R_{ss} / Ω	t_{Li+}
10	0.00361	400.76	0.00124	272.94	0.304

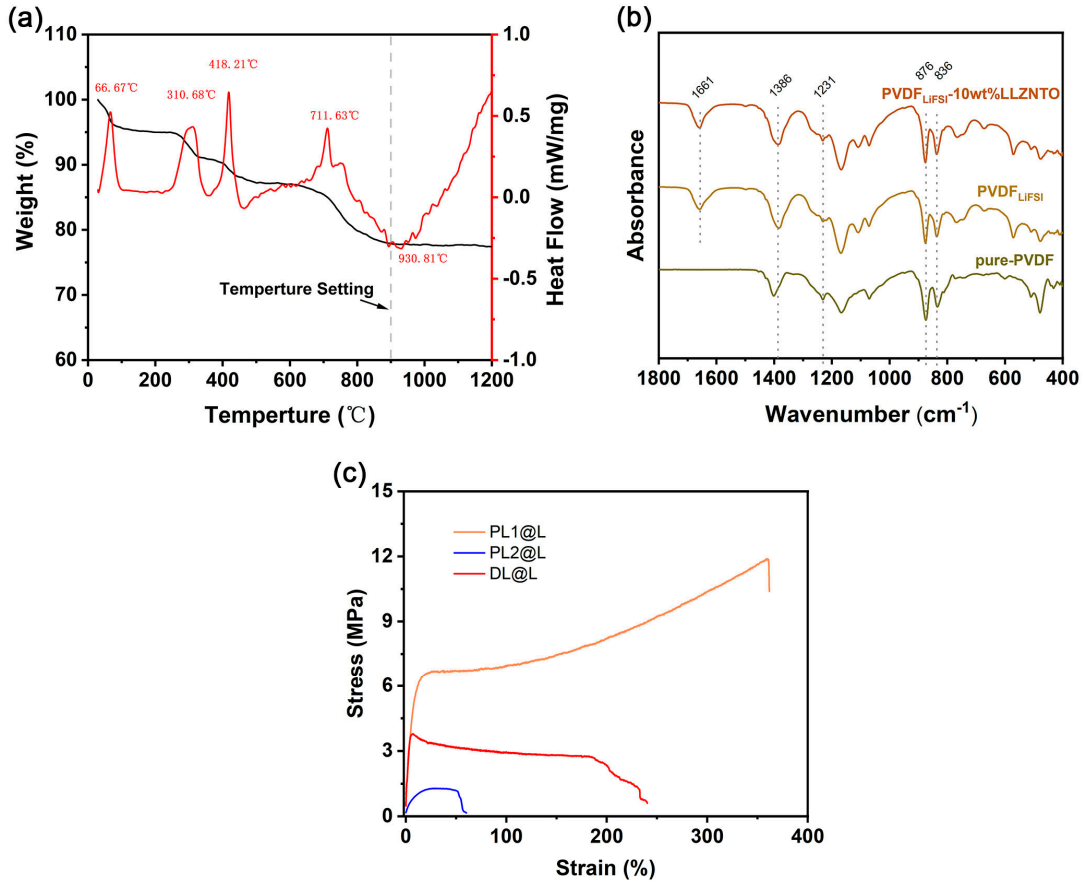

Figure S1. (a) TG-DSC curve of raw material powder mixture of LLZNTO, which suggesting the suitable synthesis temperature is between 850 ℃ and 1000 ℃; (b) FT-IR spectra of pure PVDF, PVDF with Li-salt and PL1@L; (c) Mechanical tensile stress–strain curves of PL1@L, PL2@L, and DL@L solid electrolytes.

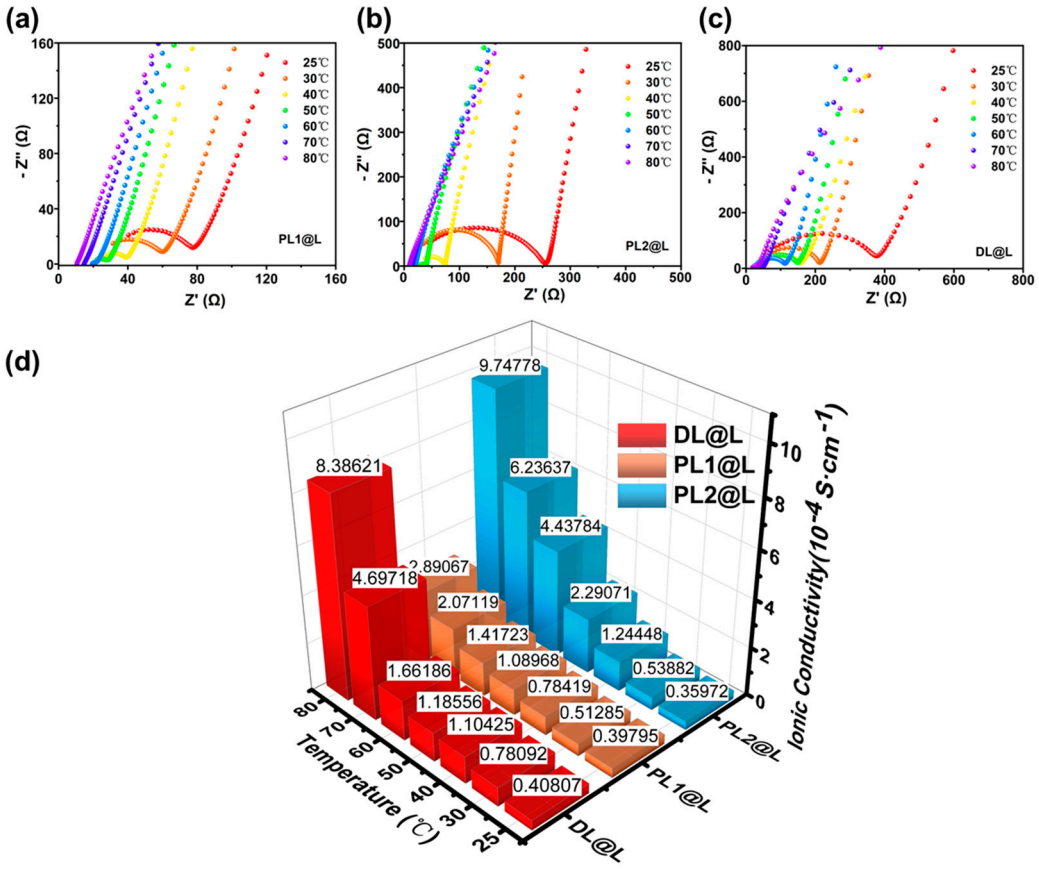

Figure S2. EIS spectra of (a) PL1@L (60 μm), (b) PL2@L (180 μm), (c) DL@L (260 μm); and (d) Ionic conductivity of PL1@L, PL2@L and DL@L at different temperature ranging from 25 to 80 °C.

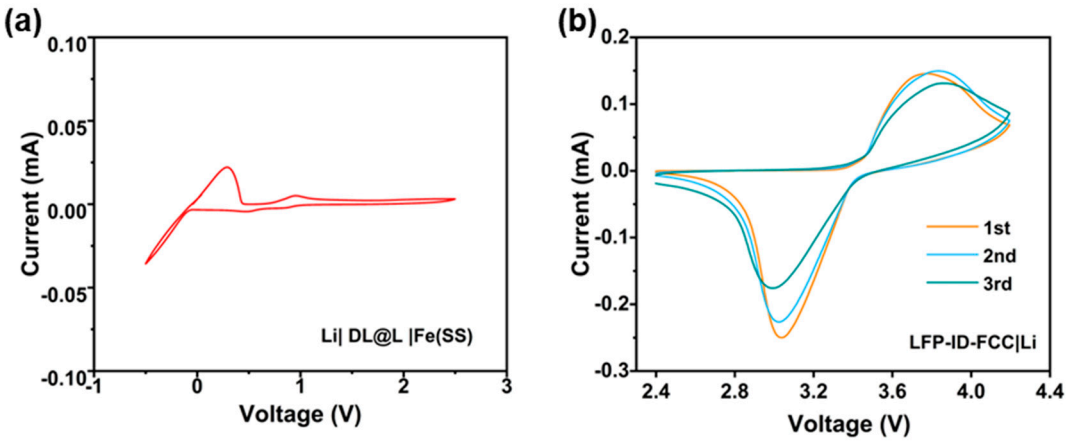

Figure S3. (a) Cyclic Voltammetry (CV) curve of the Li/DL@L/SS (stainless steel) cell from -0.5 to 2.5 V at a sweeping rate of 0.5 mV s^{-1} at 60 °C; (b) Cyclic Voltammetry (CV) curves of the LFP-ID-FCC/Li cell from 2.4 to 4.2 V at a sweeping rate of 0.1 mV s^{-1} at 60 °C.

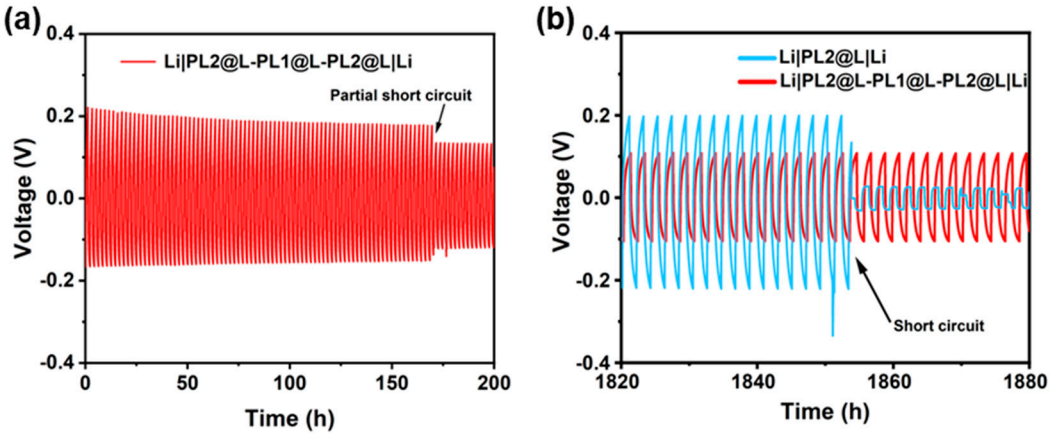

Figure S4. (a) The initial 200 cycles of voltage profile of the Li/PL2@L-PL1@L-PL2@L/Li symmetric cell at a fixed current density of 0.05 mA cm^{-2} at 60 °C; (b) Detailed voltage profiles under current densities of 0.05 mA cm^{-2} when a short circuit occurred in Li/PL2@L/Li symmetric cell.

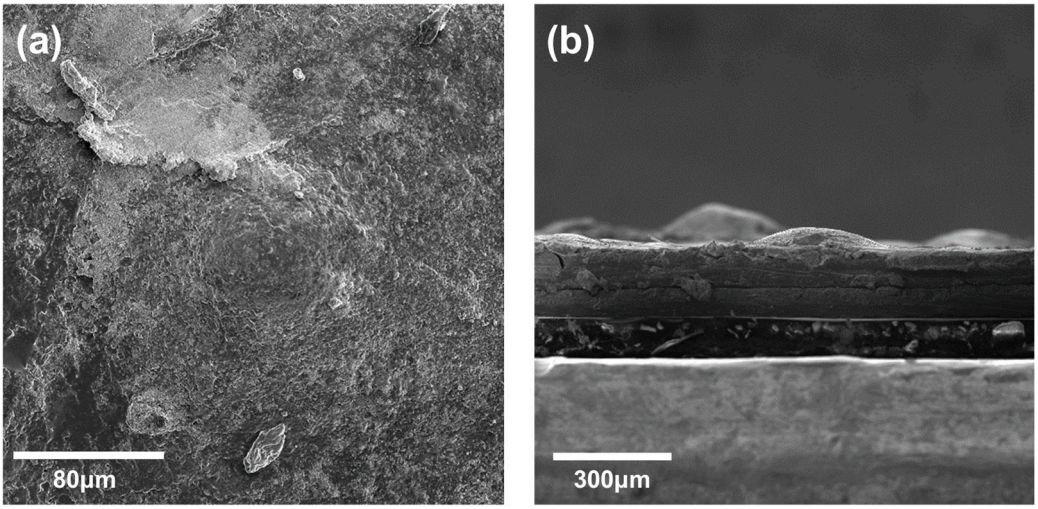

Figure S5. (a) Top-view SEM image of the surface morphology of the PL2@L layer of ID-FCC membrane after cycling; (b) Cross-sectional SEM image of ID-FCC after cycling, in which lithium-containing hills appear on the surface of ID-FCC in contact with Li.

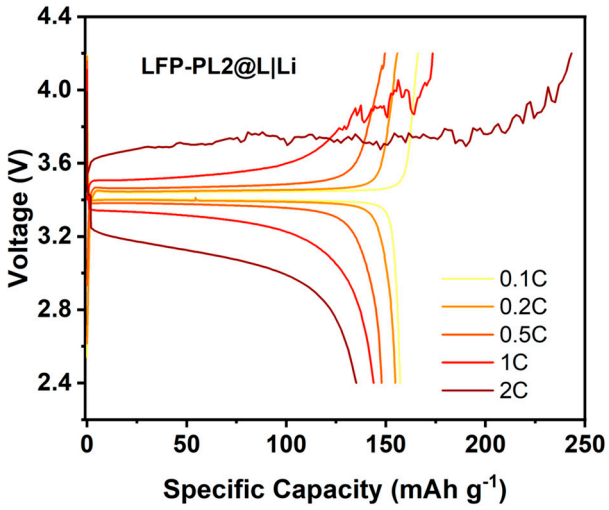

Figure S6. Galvanostatic charge–discharge voltage profiles of LFP-PL2@L/Li at the different rate.

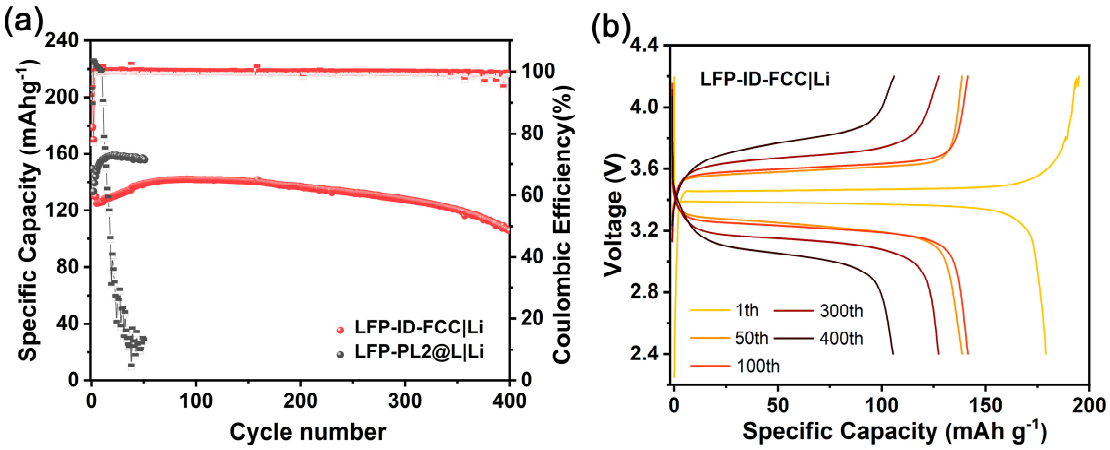

Figure S7. (a) Cycling performances of LFP-ID-FCC/Li and LFP-PL2@L/Li at 0.5 C; and (b) Galvanostatic charge–discharge voltage profiles of LFP-ID-FCC/Li at 0.5 C.

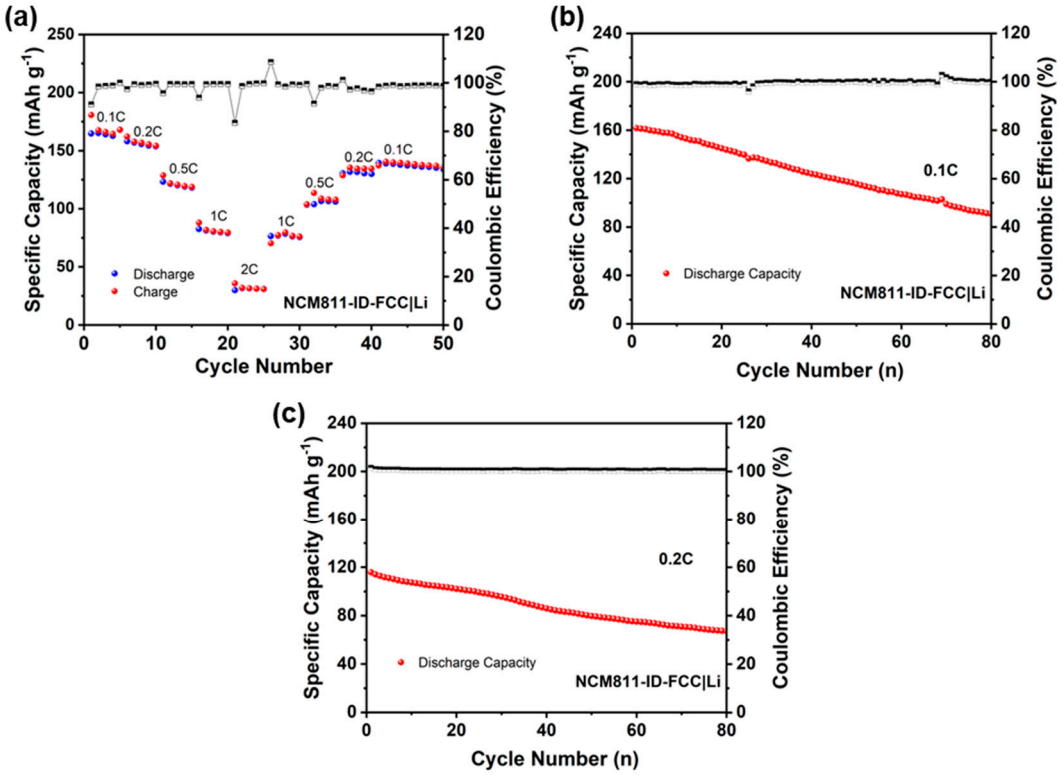

Figure S8. (a) Rate performance, (b) cycle performance at 0.1 C and (c) cycle performance at 0.2 C of NCM811-ID-FCC/Li.